

# Influence of collective effects and the d-CDW on electronic Raman scattering in high- $T_c$ superconductors

R. Zeyher<sup>a</sup> and A. Greco<sup>a,b</sup>

<sup>a</sup>Max-Planck-Institut für Festkörperforschung,  
Heisenbergstr.1, 70569 Stuttgart, Germany

<sup>b</sup>Permanent address: Departamento de Física, Facultad de Ciencias Exactas e Ingeniería and  
IFIR(UNR-CONICET), Av. Pellegrini 250, 2000-Rosario, Argentina

(October 27, 2018)

Electronic Raman scattering in high- $T_c$  superconductors is studied within the  $t - J$  model. It is shown that the  $A_{1g}$  and  $B_{1g}$  spectra are dominated by amplitude fluctuations of the superconducting and the d-wave CDW order parameters, respectively. The  $B_{2g}$  spectrum contains no collective effects and its broad peak reflects vaguely the doping dependence of  $T_c$ , similarly to the pronounced peak in the  $A_{1g}$  spectrum. The agreement of our theory with the experiment supports the picture of two different, competing order parameters in the underdoped regime of high- $T_c$  superconductors.

PACS numbers:74.72.-h, 71.10.Hf, 71.27.+a

Electronic Raman scattering in superconductors probes charge excitations across the superconducting gap and thus provides information on the magnitude and the anisotropy of the gap [1–4]. Commonly used weak-coupling theories for the interpretation of the data are, however, not able to account for the experimental spectra in the cuprates, especially, as a function of doping. Such theories yield values for the d-wave gap which have no simple relation to  $T_c$  and which are substantially smaller than those measured in ARPES experiments [5]. In our view, these problems arise because electronic correlation effects are not adequately taken into account. Below we consider a strong-coupling model which allows to consider interaction effects between excited quasi-particles as well as the appearance of a d-CDW at lower dopings in a systematic way.

Our calculations of Raman response functions are based on the widely accepted t-J model where the two spin components have been generalized to  $N$  components and the leading diagrams at large  $N$  are taken into account. As discussed in detail in Ref. [6] the phase diagram in this limit is largely determined by the onset of a flux phase with d-wave symmetry, often also called d-CDW [7], at a doping  $\delta = \delta_0$ . The corresponding order parameter has the form  $\Phi(\mathbf{k}) = -i/2N_c \sum_{\mathbf{q}\sigma} J(\mathbf{k} - \mathbf{q}) \langle \tilde{c}_{\mathbf{q}\sigma}^\dagger \tilde{c}_{\mathbf{q}+\mathbf{Q}\sigma} \rangle$ .  $J$  is the Heisenberg coupling,  $\tilde{c}^\dagger, \tilde{c}$  are creation and annihilation operators for electrons under the constraint that double occupancies of lattice sites are excluded,  $N_c$  is the number of primitive cells,  $\langle \dots \rangle$  denotes an expectation value, and  $\mathbf{Q}$  is the wave vector of the d-CDW. Furthermore, there exists for all dopings an instability towards d-wave superconductivity [8]. Keeping only the instantaneous term in the effective interaction, the order parameter is  $\Delta(\mathbf{k}) = 1/2N_c \sum_{\mathbf{q}} (J(\mathbf{k} - \mathbf{q}) - V_C(\mathbf{k} - \mathbf{q})) \langle \tilde{c}_{\mathbf{q}\uparrow} \tilde{c}_{-\mathbf{q}\downarrow} \rangle$ . As shown in Ref. [6] it is in general necessary to include the Coulomb potential  $V_C$  in order to stabilize the d-CDW with respect to phase separation. The resulting superconducting transition temperature  $T_c$  decreases

with increasing doping for  $\delta > \delta_0$ . For  $\delta < \delta_0$  the two order parameters compete with each other leading to a strongly decreasing  $T_c$  with decreasing doping. As a result optimal doping is essentially determined by  $\delta_0$ . In the presence of the two order parameters the operators  $(\tilde{c}_{\mathbf{k},\uparrow}^\dagger, \tilde{c}_{-\mathbf{k},\downarrow}, \tilde{c}_{\mathbf{k}+\mathbf{Q},\uparrow}^\dagger, \tilde{c}_{-\mathbf{k}-\mathbf{Q},\downarrow})$  are coupled leading to the following Green's function matrix [6]

$$G^{-1}(z, \mathbf{k}) = \begin{pmatrix} z - \epsilon(\mathbf{k}) & -\Delta(\mathbf{k}) & -i\Phi(\mathbf{k}) & 0 \\ -\Delta(\mathbf{k}) & z + \epsilon(\mathbf{k}) & 0 & i\Phi(\bar{\mathbf{k}}) \\ i\Phi(\mathbf{k}) & 0 & z - \epsilon(\bar{\mathbf{k}}) & -\Delta(\bar{\mathbf{k}}) \\ 0 & -i\Phi(\bar{\mathbf{k}}) & -\Delta(\bar{\mathbf{k}}) & z + \epsilon(\bar{\mathbf{k}}) \end{pmatrix} \quad (1)$$

$\epsilon(\mathbf{k})$  is the one-particle energy,  $\epsilon(\mathbf{k}) = -(\delta t + \alpha J)(\cos(k_x) + \cos(k_y)) - 2t' \delta \cos(k_x) \cos(k_y) - \mu$ , with  $\alpha = 1/N_c \sum_{\mathbf{q}} \cos(q_x) f(\epsilon(\mathbf{q}))$ .  $f$  is the Fermi function,  $\delta$  the doping away from half-filling,  $\mu$  a renormalized chemical potential,  $t$  and  $t'$  are nearest and second-nearest neighbor hopping amplitudes,  $z$  a complex frequency, and  $\bar{\mathbf{k}} = \mathbf{k} - \mathbf{Q}$ .

Expressing the expectation values in the order parameters by  $G$  and using Eq.(1) one obtains two coupled equations for the order parameters. Detailed considerations [6] show that for dopings in the neighborhood of the optimal doping  $\delta_0$  the most stable order parameters have d-wave symmetry,  $\Phi(\mathbf{k}) = \Phi\gamma(\mathbf{k})$ ,  $\Delta(\mathbf{k}) = \Delta\gamma(\mathbf{k})$ , with  $\gamma(\mathbf{k}) = (\cos(k_x) - \cos(k_y))/2$ . Fig. 1 shows the doping dependence of  $\Phi$  and  $\Delta$  at zero temperature, calculated for  $t'/t = -0.35$  and  $J/t = 0.3$ . The energy unit is  $t$ . A repulsive nearest-neighbor Coulomb interaction was also included with  $V_C/t = 0.06$ . In the overdoped region  $\delta > \delta_0$   $\Phi$  is zero and  $\Delta$  increases monotonically with decreasing  $\delta$ . After the onset of the flux phase at  $\delta_0$   $\Phi$  is first suppressed by superconductivity and then, with decreasing doping, increases steeply and suppresses now, in addition to  $V$ , the superconducting order parameter. In our calculation we assumed the value  $(\pi, \pi)$  for the wave vector  $\mathbf{Q}$ . Fig. 1 shows that superconductivity

coexists in the underdoped region with the d-CDW and that the competition between the two order parameters leads to the rapid decay of  $T_c$  towards small dopings.

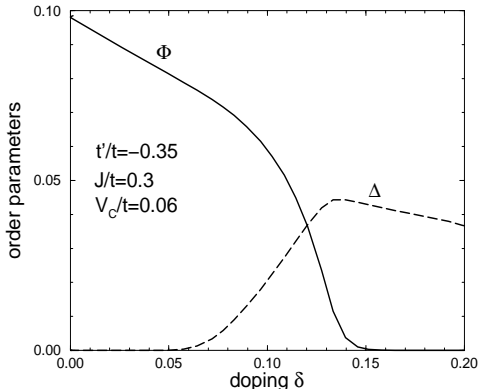


FIG. 1. Order parameters  $\Phi$  and  $\Delta$  as a function of doping in units of  $t$  at  $T = 0$ .

The scattering intensity of electronic Raman scattering is proportional to  $-(1 + n(\omega))\text{Im}\chi_\alpha(\omega + i\eta)$ , where  $n$  denotes the Bose factor,  $\omega$  the frequency, and  $\chi_\alpha$  a response function of the non-local density operator  $\rho_\alpha(\mathbf{k}) = 1/N_c \sum_{\mathbf{k}, \sigma} \gamma_\alpha(\mathbf{k}) \tilde{c}_{\mathbf{k}, \sigma}^\dagger \tilde{c}_{\mathbf{k} + \mathbf{k}, \sigma}$ .  $\alpha = 1, 3, 4$  stands for the representations  $A_{1g}, B_{1g}, B_{2g}$  of the point group  $D_{4h}$  of the square lattice, respectively. In the large  $N$  limit of the  $t$ - $J$  model we have  $\gamma_1(\mathbf{k}) = (\delta t + J\alpha)(\cos k_x + \cos k_y)/2 + 2\delta t' \cos k_x \cdot \cos k_y$ ,  $\gamma_3(\mathbf{k}) = (\delta t + J\alpha)(\cos k_x - \cos k_y)/2$ ,  $\gamma_4(\mathbf{k}) = -2\delta t' \sin k_x \cdot \sin k_y$ . The response function  $\chi_\alpha$  is determined at large  $N$  by the sum over ladder diagrams shown in Fig. 2.

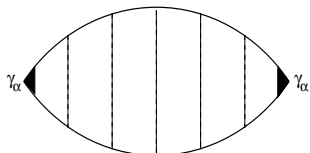


FIG. 2. Ladder diagrams for the Raman susceptibility; the filled triangle is the Raman vertex  $\gamma_\alpha$ , the solid and dashed lines represent the Green's function  $G$  and a residual interaction, respectively.

In the case of the  $B_{1g}$  and  $B_{2g}$  spectra the residual interaction is the Heisenberg interaction. Decomposing it into irreducible basis functions of  $D_{4h}$  it contains one  $B_{1g}$  kernel but no contribution with  $B_{2g}$  symmetry. This means that  $\chi_4$  is given by the free susceptibility  $\chi_4^{(0)}$  which reduces to the standard expression if the d-CDW order parameter vanishes. We find the following analytic expressions  $\chi_3(z) = \chi_3^{(0)}(z)/(1 + J'\chi_3^{(0)}(z))$ ,  $J' = J/(\delta t + J\alpha)^2$ ,  $\chi_4(z) = \chi_4^{(0)}(z)$ , with

$$\chi_\alpha^{(0)}(z) = \frac{2}{N_c} \sum_{\mathbf{k}} \gamma_\alpha^2(\mathbf{k}) \left( \Pi_{11,11}(\mathbf{k}, z) - \Pi_{12,21}(\mathbf{k}, z) \right)$$

$$+ (-1)^\alpha [\Pi_{13,31}(\mathbf{k}, z) - \Pi_{14,41}(\mathbf{k}, z)], \quad (2)$$

$$\Pi_{ij,kl}(\mathbf{k}, z) = T \sum_n G_{ij}(i\omega_n + z, \mathbf{k}) G_{kl}(i\omega_n, \mathbf{k}), \quad (3)$$

for  $\alpha = 3, 4$ .

Fig. 3 shows  $B_{1g}$  and  $B_{2g}$  spectra for the parameters  $t'/t = -0.35$ ,  $J/t = 0.3$ , and  $T = 0$ . The upper diagram, corresponding to  $\delta = 0.178$ ,  $\Delta = 0.040$  and  $\Phi = 0$ , is typical for the overdoped region. In the  $B_{2g}$  spectra  $\gamma_4$  heavily weights transitions near the diagonals in  $\mathbf{k}$ -space where the gap vanishes. As a result the spectrum is broad and peaks substantially below  $2\Delta$ . Neglecting vertex corrections  $\chi_3^{(0)}$  is determined by free particle-hole excitations mainly across the maximum of the d-wave gap. This leads to a well-pronounced peak at  $2\Delta$  as shown by the dashed curve in the upper diagram of Fig.3. Including also vertex corrections  $\chi_3$  develops a bound state well within the d-wave gap which is somewhat broadened by the finite density of states in the d-wave gap. Practically all spectral weight is shifted from the region around and above  $2\Delta$  into the bound state which, in analogy to semiconductors, can be viewed as an exciton state [9].

The middle and lower diagrams in Fig. 3 describe a slightly and a strongly underdoped case, respectively. In the extreme case of  $\Phi \gg \Delta$  the density of quasi-particles shows a small gap due to superconductivity embedded into a larger gap structure due to the flux phase. The  $B_{2g}$  spectra (dotted lines) are always very broad with a maximum which is located roughly in the middle of the BCS-gap which decreases with decreasing doping. In addition it contains a weak and structureless background which extends over the whole gap region. The dashed lines in Fig. 3 describe the  $B_{1g}^{(0)}$  spectrum due to non-interacting particle-hole excitations. It is rather insensitive to the BCS-part of the gap and consists of one strong peak around the maximal total gap. Taking also vertex corrections into account practically the total spectral weight of the  $B_{1g}^{(0)}$  curve is shifted into one peak which monotonically increases with decreasing doping. It describes amplitude fluctuations of the d-CDW order parameter.

The essential features of Fig.3 agree with experiments in the cuprates, in particular, the increase of the frequency of the  $B_{1g}$  peak with decreasing doping and the nonmonotonic behavior of the  $B_{2g}$  peak as a function of doping similar to that of  $T_c$  [3]. Quantitative fits to experimental curves [10] need, however, the inclusion of additional interactions, e.,g., with impurities, and are therefore not attempted here. To what extent the predicted large excitonic effect in the  $B_{1g}$  spectrum is compatible with experiment is presently unclear: The larger gap values deduced from ARPES data in comparison to the Raman  $B_{1g}$  peak in the

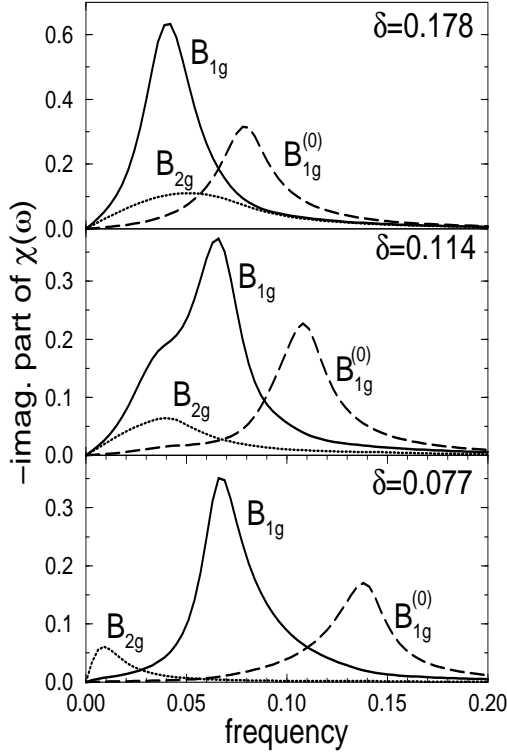


FIG. 3. Electronic Raman spectra of B-symmetry for three different dopings  $\delta$ , calculated for  $t'/t = -0.35$ ,  $J/t = 0.3$ , and  $T = 0$ . The  $B_{2g}$  spectrum has been multiplied by 10 in the two upper and by 100 in the lower diagrams.

underdoped regime and the small difference between  $B_{1g}$  and  $B_{2g}$  peaks on the overdoped side are in favor of excitonic effects in the  $B_{1g}$  channel. ARPES gives in slightly overdoped  $Bi2212$   $2\Delta \sim 70 - 75 meV$  [5] whereas the  $B_{1g}$  peak lies near  $59 - 63 meV$  [1,4], for the same doping. ARPES yields in untwinned  $YBa_2CuO_7$  gaps of 58 and 88 meV at the  $X$  and  $Y$ -points, respectively [11], whereas the corresponding peaks in Raman scattering are at 50 and 60 meV [12]. Excitonic effects in the  $B_{1g}$  channel thus seem not to be in conflict with available data. The overall decrease in intensity as a function of doping of the theoretical B-spectra is mainly caused by the  $\delta^2$  factor in the Raman vertices. It agrees with experiment, however, the experimental  $B_{1g}$  spectrum decreases faster than the  $B_{2g}$  spectrum in contrast with the theoretical curves.

The dotted lines in Fig. 4, called  $A_{1g,s}$ , show screened  $A_{1g}$  spectra. Their absolute intensities are about 2 orders in magnitude smaller than those for  $B_{1g}$  scattering. Moreover, they show in general two gap features, a weaker one related to the BCS and a stronger one reflecting the total gap. All these features clearly indicate that the  $A_{1g,s}$  curves are unable to explain the experimental  $A_{1g}$  spectra.

According to Ref. [13] density fluctuations may couple to the superconducting order parameter via the modulation of the density of states at the Fermi energy. This

indirect coupling also applies to the density fluctuations induced by the  $A_{1g}$  Raman vertex  $\gamma_1$ . Using the BCS-assumption with a cutoff  $\omega_0$  the effective Raman coupling is  $\sum_{\mathbf{k}} \tilde{\gamma}_1(\mathbf{k}) \tilde{c}_{\mathbf{k}\uparrow}^\dagger \tilde{c}_{-\mathbf{k}\downarrow}^\dagger + \text{h.c.}$ , with  $\tilde{\gamma}_1 = g\gamma_1(\mathbf{k})$  and  $g = \Delta \ln(\omega_0/\Delta) \delta N(0)/N(0)$ , where  $\delta N(0)$  is the change in the projected d-wave density at the Fermi surface due to the original Raman vertex  $\gamma_1$ . The effective vertex  $\tilde{\gamma}_1$  is unscreened. Moreover,  $g$  is large in the optimal and overdoped region because of the proximity of the van Hove singularity which enhances  $\delta N(0)$  and decays rapidly in the underdoped region because of the factor  $\Delta$ . The resulting  $A_{1g}$  spectrum is again given by the diagram in Fig. 2 with external Raman vertices  $\tilde{\gamma}_1$  and the Heisenberg interaction for the dashed line. Denoting the resulting susceptibilities with a tilde we obtain  $\tilde{\chi}_1(z) = \tilde{\chi}_1^{(0)}(z)/(1 + J\tilde{\chi}_1^{(0)}(z)/g^2)$ ,

$$\tilde{\chi}_1^{(0)}(z) = \frac{g^2}{N_c} \sum_{\mathbf{k}} \gamma^2(\mathbf{k}) (\Pi_{12,12}(\mathbf{k}, z) + \Pi_{11,22}(\mathbf{k}, z) - \Pi_{14,32}(\mathbf{k}, z) - \Pi_{13,42}(\mathbf{k}, z) + (z \rightarrow -z)). \quad (4)$$

The dashed and solid lines in Fig. 4, denoted by  $\tilde{A}_{1g}^{(0)}$  and  $\tilde{A}_{1g}$ , show the negative imaginary part of  $\tilde{\chi}_1^{(0)}$  and  $\tilde{\chi}_1$ , respectively, for the same three dopings as in Fig. 3, calculated with the cutoff  $\omega_0 = J$ .  $\tilde{A}_{1g}^{(0)}$  exhibits a step-like feature at  $2\Delta$  in the overdoped regime which transforms into a well-pronounced peak towards lower dopings. The peak coincides with the maximum of the total gap and there is no indication of any contribution from the smaller BCS gap, similar as in the  $B_{1g}^{(0)}$  spectrum. Including also vertex corrections spectral weight around  $2\Delta$  accumulates into a pronounced collective peak at  $2\Delta$  in the overdoped region describing amplitude fluctuations of the superconducting order parameter [13]. Going from the overdoped to the underdoped regime this peak first increases, then passes through a maximum around optimal doping, and then decreases in frequency and intensity, becoming at the same time rather broad. The decrease in its frequency can easily be understood: The denominator of  $\tilde{\chi}_1(z)$  becomes zero at zero frequency in the limit  $\Delta \rightarrow 0$  if  $\Delta$  satisfies the gap equation. This implies that the frequency of the collective peak in  $\tilde{\chi}_1(z)$  has to go to zero at the onset of superconductivity in the underdoped region in the absence of damping. The density of states is, however, nonzero in the d-CDW gap even at low frequency. As a result, the collective peak varies as  $2\Delta$  at larger energies but becomes rather broad at low energies. This agrees with experiments in  $Bi2212$  where the  $A_{1g}$  peak passes through a maximum and then decreases on the underdoped side [1]. Taking also data on phonon renormalizations into account it even has been conjectured [2] in the case of  $YBa_2Cu_3O_7$  that the  $A_{1g}$  peak corresponds to the superconducting gap  $2\Delta$ .

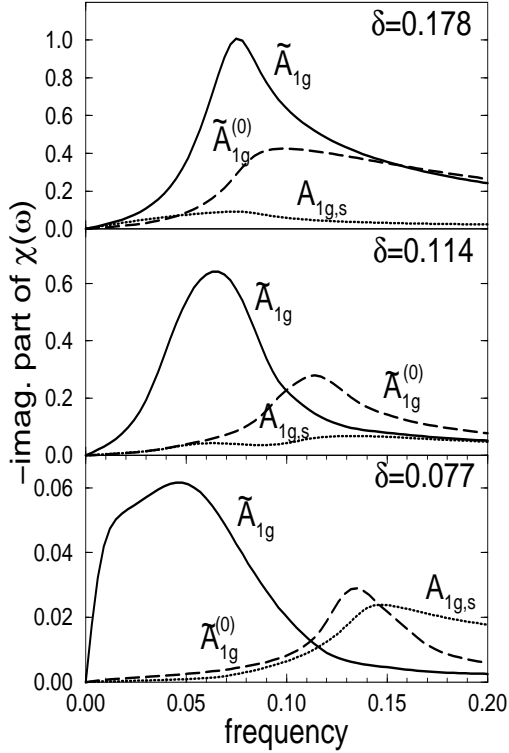


FIG. 4.  $\tilde{A}_{1g}^{(0)}$  and  $\tilde{A}_{1g}$ : Unperturbed and full  $A_{1g}$  spectra calculated with the indirect coupling;  $A_{1g,s}$ : Screened, full  $A_{1g}$  spectrum multiplied by 50 (upper two diagrams) or 10 (lower diagram).

Fig. 4 shows that  $\tilde{A}_{1g}$  is much larger in magnitude than  $A_{1g,s}$  for all dopings, in spite of the fact that the coupling to the superconducting order parameter occurs in an indirect way. One reason is that the  $\tilde{\gamma}_1$  vertex is un-screened in contrast to  $\gamma_1$  and that screening reduces the intensity by one order of magnitude or more. A second reason is that the proximity to the van Hove singularity leads to rather large values for  $\delta N(0)/N(0)$  between 2 and 5 in the considered doping region. Comparing the theoretical intensities for  $B_{1g}$  and  $\tilde{A}_{1g}$  scattering with the experimental ones one finds that  $\tilde{A}_{1g}$  has the right magnitude whereas  $A_{1g,s}$  would be much too small. We would like to point out, however, that the coupling constant  $g$  also depends on the cutoff  $\omega_0$  and thus is subject to considerable uncertainty.

In conclusion, we have shown that the observed different behavior of the three symmetry components of the electronic Raman spectrum in high- $T_c$  superconductors

as a function of doping can be explained within a t-J model in the large N limit. Basic ingredients of this approach are the strong competition of the superconducting and the d-CDW order parameters in the underdoped regime and the importance of collective effects. The peak in the  $B_{1g}$  spectrum in the superconducting state is explained by amplitude fluctuations of the d-CDW order parameter which, in the optimal and overdoped region, can also be viewed as excitonic states. We also found that the indirect coupling of light to the superconducting order parameter is important leading to the conclusion that the  $A_{1g}$  peak is caused by amplitude fluctuations of the superconducting order parameter.

The authors thank Secyt and the BMBF (Project ARG 99/007) for financial support and C. Bernhard for a critical reading of the manuscript.

- 
- [1] C. Kendziora and A. Rosenberg, Phys. Rev. B **52**, R9867 (1995)
  - [2] T. Strohm and M. Cardona, Phys. Rev. B **55**, 12725 (1997)
  - [3] M. Opel, R. Nemetschek, C. Hoffmann, R. Philipp, P.F. Müller, and R. Hackl, Phys. Rev. B **61**, 9752 (2000)
  - [4] F. Venturini, M. Opel, R. Hackl, H. Berger, L. Forro, and B. Revaz, cond-mat/0110439
  - [5] M.R. Norman, H. Ding, J.C. Campuzano, T. Takeuchi, M. Randeria, T. Yokoya, T. Takahashi, T. Mochiku, and K. Kadowaki, Phys. Rev. Lett. **79**, 3506 (1997)
  - [6] E. Cappelluti and R. Zeyher, Phys. Rev. B **59**, 6475 (1999)
  - [7] S. Chakravarty, R.B. Laughlin, D.K. Morr, and Ch. Nayak, Phys. Rev. B **63**, 94503 (2001)
  - [8] R. Zeyher and A. Greco, Eur. Phys. J B **6**, 473 (1998)
  - [9] A.V. Chubukov, D.K. Morr, and G. Blumberg, Sol. State Comm. **112**, 183 (1999)
  - [10] T.P. Devereaux and A.P. Kampf, Phys. Rev. B **61**, 1490 (2000)
  - [11] D.H. Lu, D.L. Feng, N.P. Armitage, K.M. Shen, A. Damascelli, C. Kim, F. Ronning, Z.-X. Shen, D.A. Bonn, R. Liang, W.N. Hardy, A.I. Rykov, and S. Tajima, Phys. Rev. Lett. **86**, 4370 (2001)
  - [12] M.F. Limonov, A.I. Rykov, S. Tajima, and A. Yamanaka, Phys. Rev. B **61**, 12412 (2000)
  - [13] P.B. Littlewood and C.M. Varma, Phys. Rev. Lett. **47**, 811 (1981)